Stand-Alone and Hybrid Electric Thermal Energy Storage in the System Advisor Model

Ty Neises, Bill Hamilton, Janna Martinek, and Joshua McTigue

National Renewable Energy Laboratory

NREL is a national laboratory of the U.S. Department of Energy
Office of Energy Efficiency & Renewable Energy
Operated by the Alliance for Sustainable Energy, LLC

This report is available at no cost from the National Renewable Energy Laboratory (NREL) at www.nrel.gov/publications.

Contract No. DE-AC36-08GO28308

Technical Report
NREL/TP-5700-82989
July 2022

Stand-Alone and Hybrid Electric Thermal Energy Storage in the System Advisor Model

Ty Neises, Bill Hamilton, Janna Martinek, and Joshua McTigue

National Renewable Energy Laboratory

Suggested Citation
Neises, Ty, Bill Hamilton, Janna Martinek, and Joshua McTigue. 2022. *Stand-Alone and Hybrid Electric Thermal Energy Storage in the System Advisor Model*. Golden, CO: National Renewable Energy Laboratory. NREL/TP-5700-82989. https://www.nrel.gov/docs/fy22osti/82989.pdf.

NREL is a national laboratory of the U.S. Department of Energy
Office of Energy Efficiency & Renewable Energy
Operated by the Alliance for Sustainable Energy, LLC

This report is available at no cost from the National Renewable Energy Laboratory (NREL) at www.nrel.gov/publications.

Contract No. DE-AC36-08GO28308

Technical Report
NREL/TP-5700-82989
July 2022

National Renewable Energy Laboratory
15013 Denver West Parkway
Golden, CO 80401
303-275-3000 • www.nrel.gov

NOTICE

This work was authored by the National Renewable Energy Laboratory, operated by Alliance for Sustainable Energy, LLC, for the U.S. Department of Energy (DOE) under Contract No. DE-AC36-08GO28308. Funding provided by the U.S. Department of Energy Office of Energy Efficiency and Renewable Energy Solar Energy Technologies Office. The views expressed herein do not necessarily represent the views of the DOE or the U.S. Government.

Preface

This report represents the final project deliverable for the project, "Performance Modeling and Dispatch Optimization in SAM of Hybrid Concentrating Solar Power Electric Thermal Energy Storage and Stand-Alone Electric Thermal Energy Storage Systems," under U.S. Department of Energy award #37870. The project period was from December 1, 2020, through March 31, 2022.

This report first describes the motivation and methodology for modeling electric thermal energy storage (both stand-alone and hybrid). Then the report discusses comparison of dispatch results to PLEXOS and availability of the models in the System Advisor Model.

Acknowledgments

The authors would like to thank the Concentrating Solar-Thermal Power team at the U.S. Department of Energy's Solar Energy Technologies Office for funding this project, and Andru Prescod in particular for his technical guidance.

List of Acronyms

COP	coefficient of performance
CSP	concentrating solar power
ETES	electric thermal energy storage
HTF	heat transfer fluid
IRR	internal rate of return
LCGS	low-carbon grid scenario
LCOE	levelized cost of energy
LCOS	levelized cost of storage
LMP	locational marginal electricity price
MSPT	molten-salt power tower
O&M	operation and maintenance
PPA	power purchase agreement
SAM	System Advisor Model
SSC	SAM's simulation core
TES	thermal energy storage
UI	user interface

Executive Summary

Dispatch optimization of system operations, through maximizing revenue subject to system constraints, is essential to evaluate the economic value of a particular system design, but there is a lack of neutral third-party, publicly available, open-source models to evaluate the performance, dispatch, and financial viability of these systems. Therefore, this project developed performance and dispatch optimization techno-economic models for:

1. Stand-alone electric thermal energy storage (ETES)
2. Stand-alone pumped thermal energy storage (PTES)
3. Hybrid molten-salt power tower (MSPT) + ETES.

The models are available to the public through the System Advisor Model (SAM) software, scripting, and as open-source code. We also have a complementary journal article [4] under review that details the ETES dispatch model methodology and demonstrates model functionality.

We compared results of the dispatch model to the PLEXOS dispatch of a similar generator using the same initial grid pricing signal and found our dispatch model performed well, but closer agreement between the models was limited by the inherent differences between price-taker (SAM) and unit commitment (PLEXOS) models. Nevertheless, the price-taker models developed in this project are useful to analyze proposed ETES and PTES technologies because they provide more detailed system and component models, solve orders-of-magnitude faster, and are available as free open-source software. The model results represent the most optimistic returns considering grid arbitrage from the input electricity pricing, so the financial results can be applied as a feasibility stage-gate for system designs and pricing scenarios of interest.

Table of Contents

List of Figures

List of Tables

1 Background

Dispatchable systems derive value from their ability to store energy when prices are low and generate electricity when prices are favorable—i.e., energy arbitrage. Consequently, dispatch optimization of system operations, through maximizing revenue subject to system constraints, is essential to evaluate the economic value of a particular system design. The National Renewable Energy Laboratory (NREL) recently developed a molten-salt power tower (MSPT) dispatch model for concentrating solar power (CSP) that improves power purchase agreement (PPA) price 10%–15% versus the previous heuristic dispatch model for electricity pricing schedules that contain morning and afternoon price peaks [1]. The model achieves this improvement by precisely balancing charging storage for use during high-value time periods with maintaining enough charging margins to minimize solar field curtailment. Furthermore, the analysis shows that dispatch optimization alters the optimal plant design by changing the optimal size of thermal energy storage (TES) and solar multiple from those values found without dispatch optimization. For dispatchable systems that can charge storage using grid electricity, it is likely more important to optimize operation under different grid pricing scenarios.

Although hybrid MSPT-ETES and stand-alone ETES technologies offer potential advantages as dispatchable grid storage technologies, there is a lack of neutral third-party, publicly available, open-source models to evaluate the performance, dispatch, and financial viability of these systems. One option is a grid commitment model like PLEXOS [2], a commercial software package that models all generators and storage devices on the grid interconnect and dispatches them to minimize the cost of generation. However, PLEXOS must represent an expansive set of devices, off-takers, and transmission lines, which requires: (1) simplified technology models, (2) user expertise, and (3) large computational resources and time. While researchers at NREL have used PLEXOS to understand trade-offs between high level hybrid ETES design parameters, it is not an ideal tool for widespread adoption. Another option to model stand-alone ETES performance and dispatch is to use a model developed for electrochemical batteries. This approach is inadequate because ETES systems have different design parameters and operational constraints than batteries**.** Furthermore, dispatch optimization of batteries also is a separate area of ongoing research.

ETES systems often use levelized cost of storage (LCOS) as a figure of merit that can include capital costs, operation and maintenance (O&M) costs, and optionally the estimated average cost of electricity necessary to charge the system. However, LCOS does not account for the time value of electricity during charge and discharge, which heavily influences the financial viability of the system. For example, a system design with low capital cost and low round-trip efficiency (e.g., 40%) may have the same LCOS as a system design with high capital cost and high round-trip efficiency (e.g., 60%). The proposed model will show how each of these systems optimally operates over a grid-pricing schedule. As a simple example, consider a two-tier grid-pricing schedule where the highest price is twice the lowest price. In this scenario, the system with the 40% round trip efficiency can only earn in electricity sales 80% of the total cost of input electricity, so, regardless of its capital cost, it cannot generate positive revenue. In contrast, the system with the 60% round trip efficiency can earn in electricity sales 120% of the total cost of input electricity.

Hybrid CSP-ETES systems further complicate the usefulness of LCOS as a figure of merit. CSP analyses typically report metrics that use the cumulative electricity the plant generates or cumulative electricity sales to account for day-to-day and seasonal variations in plant performance. Consequently, it is difficult to use LCOS to understand the viability of integrating an ETES design with CSP. Furthermore, CSP systems, once constructed, typically have low operational costs to charge TES and, compared to ETES, tend to favor designs with larger cycle capacity factors. Finally, power cycle O&M costs are partially a function of their operational schedule (e.g., the number of startup and ramping events). NREL research has shown dispatch optimization can improve the net revenue of a MSPT system by over 5% by reducing startups and ramp rates [3].

2 Project Objective

This project developed dispatch optimization models within the SAM framework for (1) a hybrid MSPT and electric resistance ETES system, (2) a hybrid MSPT with a PTES system, (3) a stand-alone electric resistance ETES system, and (4) a stand-alone system PTES system. These models calculate annual techno-economic performance by optimizing the operating profile that maximizes electricity sales less maintenance and replacement costs caused by operation and cycling given user-input design parameters and temporal grid electricity prices. We validated the resulting dispatch model against PLEXOS modeling of a similar system. Finally, our forthcoming peer-reviewed journal article [4] describes methodology and results, and we will include the models in SAM releases. Project milestones are outlined in Table 1.

Table 1. Project Milestone Information

Page numbers refer to the initial page where information can be found in this report.

	Metric Definition	Success Value	Measured Value	Assessment Tool (Quality Assurance)	Goal Met?
1.1.1	Collect feedback from industry partners on proposed project plan	At least 2 ETES developers agree model approach is acceptable to represent their technology.	Feedback sent in FY21 Q2 report	Documented feedback sent to DOE.	Yes
1.1.2	Demonstrate <10% difference in calculated annual net revenue between the model and PLEXOS for baseline electric-resistance hybrid and stand-alone cases	<10%	Stand-alone = 10% Hybrid = 4%	PLEXOS	Yes pg. 16
1.1.3	Publish journal article describing model methodology	Record of submission	Paper submitted to *Applied Energy* on 3/16/2022	Record of submission sent to DOE along with copy of draft paper.	Yes [4]
PEC 1.3.2	Include developed models in the SAM 2021 fall release	Beta version of SAM	ETES model in 2021.12.02 release. CSP-hybrid and stand-alone PTES models sent to DOE in Beta SAM release*	Beta version containing ETES models sent to DOE	Yes pg. 35
* SAM version 2021.12.02 was released before the end of this project, and we had not completed the hybrid and PTES models before the release. The models currently are available in the Develop branch of the NREL's SAM and SSC public GitHub repositories and available as Beta versions upon request. The models will be in the next SAM release.					

3 Project Results and Discussion

3.1 Modeling Infrastructure Improvements

We modified the detailed system model framework to represent the system operating mode setup and iteration in a polymorphous class-based approach. This replaces our previous approach that hardcoded similar method calls for every unique operating mode. The new framework modularizes an important piece of the system model and enables us to add operating models faster and more accurately. We used this framework to quickly add new operating modes that include both a solar field and electric heater for the CSP-ETES hybrid model that is described in more detail in the following sections. We also migrated system dispatch and control routines to encapsulated methods that require independent variables as input arguments rather than implicitly inputting them as class member data. This approach clarifies to users which variables the methods are using and ensures that added input variables are considered in the upstream code. This modification also moved these routines out of the main block of code that solves for plant timeseries performance, which helps users better understand the model.

3.2 ETES System Model

An electric-resistance heater is a simple concept to model for the purposes of a steady-state performance model that does not require physical component dimensions. We set as model inputs the heat transfer fluid (HTF) inlet temperature (provided by the TES component model), target outlet temperature, and target heat output. Then, the model solves for the required HTF mass flow. We decided to neglect modeling the pump in our initial implementation because the electric power required by the pump is converted to heat the same as the heater electric power. The more interesting challenge was designing the component model to integrate with our existing CSP plant controller and solver methods. The CSP framework contains parent classes for the main plant components: collector-receiver, TES, and power cycle. The parent classes define information flow and template methods that are common across different technology options for that component. For example, we have power tower and trough derived (or "child") classes for the collector-receiver class. Each derived class defines detailed, technology-specific calculations for the function template provided by the parent class. The controller and solver only "see" the template information provided by the parent class, so they do not have information about the derived class they are calling for any given system simulation. As such, understanding the template function requirements and how the controller and solver use the functions is crucial to adding new technology component models to the framework.

Table 2. ETES System Design Parameters for Timeseries Simulation Using Simple Dispatch Heuristic, With Results in Figure 1

Gross cycle output (MWe)	115
Cycle efficiency (%)	41.2
Heater multiple (-)	2.4
Hours of TES (hr)	10

The main template functions required for the heater include:

- "startup": This method tracks startup energy and time (i.e., ramping) requirements and returns the required startup time to the plant solver. We currently model the startup energy requirement as an electric load and do not consider interactions with TES during startup.

- "on": This method calculates the HTF mass flow rate and outlet temperature that the collector-receiver generates, assuming all startup requirements have been satisfied. Derived classes representing CSP technologies use concentrated direct normal irradiance to heat the HTF, so their heat input is not controllable. (They can defocus if necessary to reduce input heat, but this is generally not a preferred operating state and usually applied as a reactive control. They do not have the ability to generate more heat than the time-dependent limits of direct normal irradiance and solar field optical efficiency.) In contrast, at any time the heater can control its output to any point between its maximum and minimum rating. As such, we added an input to the "on" method that represents the target collector-receiver heat output. Collector-receiver defocus driven by system constraints (e.g., full TES) is applied on top of this new input. Existing solar-driven derived classes ignore this new input.

- "estimates": This method estimates the collector-receiver performance for either startup or operating behavior, depending on operating state. The plant controller calls this method at the beginning of each timestep and uses the outputs to choose a plant operating mode to send to the solver. The initial motivation for this method was to provide a computationally simpler method to estimate collector-receiver performance as an alternative to calling "startup" or "on" methods that may be more detailed. The heater model estimates performance using the design point thermal power.

- "off": This method calculates performance when the collector-receiver component does not have a heat input and is not delivering hot HTF to the TES or cycle. For steady-state models like the heater or nominal power tower, "off" does not contain thermodynamic or heat transfer relationships and only adjusts startup requirements as necessary. For transient models like the parabolic trough or detailed power tower model, "off" models recirculated HTF, heat losses, and receiver material temperatures as a function of time.

With a fully defined collector-receiver derived class representing the heater, we can configure a nominal system model by using this derived class and the TES and cycle classes from the MSPT model. The remaining step is to provide to the plant controller operating logic specific to the ETES system. First, we need to define the collector-receiver target heat output (discussed in the "on" method description above), which we nominally fix to the design value each timestep (dispatch optimization may vary this input over time to maximize heat generation during the lowest pricing periods). Next, we need to apply logic that prohibits the collector-receiver and power cycle from simultaneously operating (which is illogical for ETES but common for solar). Finally, we need to create a simple operating heuristic and grid pricing schedule to exercise the system model before integrating rigorous dispatch optimization methods. We made a binary "square wave" pricing schedule where morning pricing multipliers are <1 and afternoon pricing multipliers >1, and we implemented operating logic that instructs the plant to try to charge whenever the price is <1 and to try to discharge whenever the price is >1.

Table 2 shows a nominal ETES system design based on the SAM's MSPT default case. Figure 1 shows the first 24 hours of a timeseries simulation using the square wave pricing schedule and simple heuristic dispatch. The first hour shows the heater starting up and then sending hot HTF to TES. From 4:00–5:00 the heater "defocuses" so that TES is filled at the end of the hour. After TES is fully charged, the plant turns off the heater and remains idle until 12:00, when the pricing switches to a multiple greater than 1. From 12:00–13:00 the cycle first starts up and then generates power. The cycle generates full load until 21:00. From 21:00–22:00 the cycle generates part load to fully deplete TES at the end of the timestep. The results show expected component and system behavior for the simple pricing schedule and heuristic control. This system is designed with a 2.4 heater multiple, so the magnitude of electric power consumed by the heater is much larger than the electric power generated by the cycle.

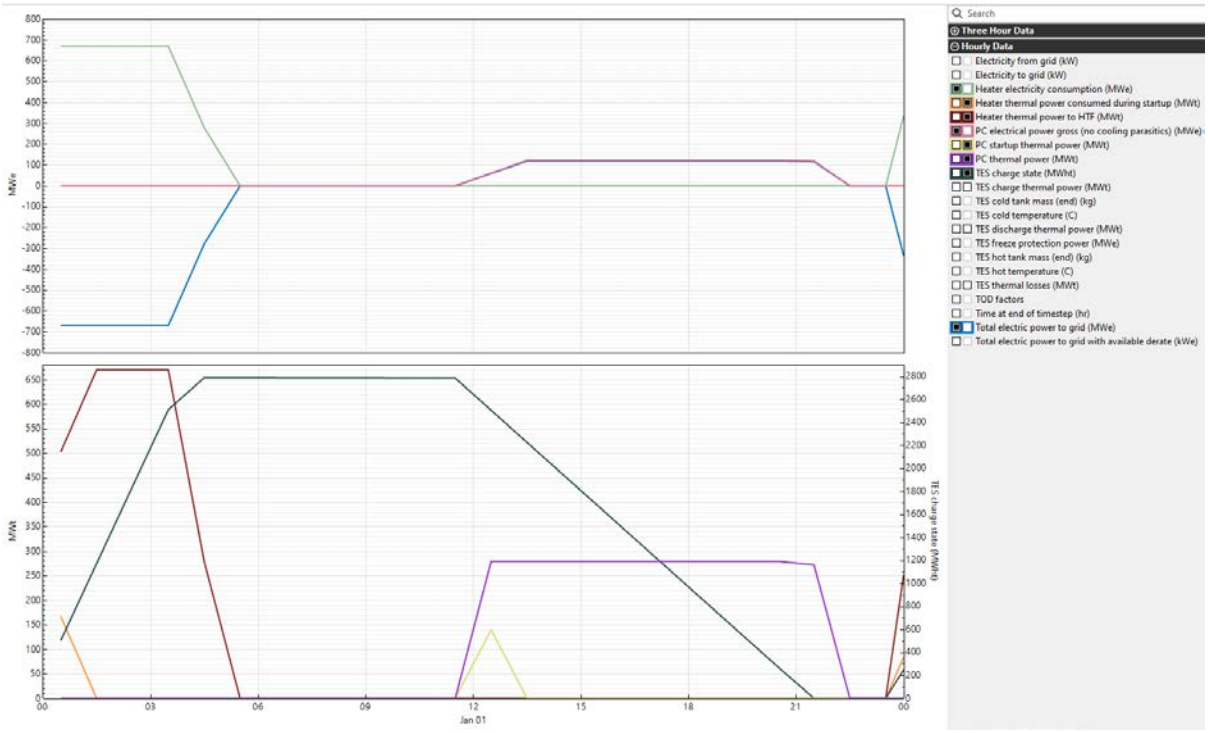

Figure 1. Electric-resistance ETES timeseries outputs using simple square wave pricing schedule and heuristic dispatch

All figures created by NREL.

3.3 ETES Dispatch Optimization

3.3.1 Dispatch Optimization Formulation

This section presents a summary of the ETES dispatch optimization formulation. Please refer to our journal submission [4] for the complete ETES dispatch optimization mathematical formulation with brief descriptions of each parameter, variable, and constraint. This work borrows and expands on our past CSP dispatch optimization work [1]. Unlike heuristic-based approaches, our dispatch optimization model ensures that the ETES system will only operate during periods that are most profitable. This can result in periods where the ETES system

operates less frequently due to less electricity price volatility. This behavior has been observed using our dispatch model and will be described in greater detail in the following results section.

The ETES dispatch optimization model determines system thermal and electrical power flows that maximize system profits, which we have defined as the difference between electricity sales and purchases, over a given time horizon. Additionally, we formulated the ETES objective to include ramping and startup financial costs for the power cycle and electric heaters. By including these operating costs, the dispatch optimization model can evaluate the tradeoff between cost of starting up and ramping the power cycle and the revenue provided by those operations. In previous work, we have used this method to eliminate detrimental price chasing behavior that could cause excessive wear and tear on system components [1].

Our ETES energy arbitrage dispatch optimization model is subject to: (1) electric heater and power cycle startup energy requirements, (2) electric heater and power cycle thermal power bounds when operating, (3) power cycle part-load efficiency curve, (4) power cycle minimum up- and down-times, (5) TES energy balance, and (6) binary logic governing modes (e.g., electric heaters and power cycle cannot operate simultaneously). The ETES performance and dispatch model uses a rolling-time horizon approach where the dispatch problem solves over a look-ahead horizon and the ETES performance model uses the dispatch solution for a subset horizon before the dispatch model is reinitialized and resolved. The look-ahead horizon sets the number of hours the model looks into the future to solve operational decisions. The model uses perfect forecasting to determine the electricity prices and ambient temperatures for the look-ahead horizon, which it reads from the annual time-series data provided by the user. The ETES model requires the ambient temperature for the power cycle performance adjustment and the cycle cooler parasitic losses. For each dispatch solve, the dispatch problem parameters are initialized by the design values and initial states (e.g., the TES state of charge) of the system to sync the dispatch model to the performance model.

3.3.2 Dispatch Optimization Results

Note that the results in this section are preliminary and demonstrate the main capabilities and outcomes of the ETES dispatch model—our journal paper contains updated results using the most recent code that contains minor improvements. To exercise the dispatch optimization model, we conducted a parametric study varying hours of TES and heater multiple. The latter is defined as ratio of the electric heater thermal rating over the thermal capacity of the power cycle, similar to solar multiple defined for CSP systems. We used the MSPT SAM module default cycle size and efficiency for this study, which is 115 MWe gross and 41.2%, respectively. For hours of storage and heat multiple, we evaluated a full-factorial design over a range of 4 to 20 hours of storage at a 2-hour interval and a heater multiple range of 1 to 4 at a 0.5 interval, resulting in 63 samples. For the market price signal, we used normalized prices from the 2030 "Target high solar" California PLEXOS scenario shown in Figure 2 as a time of the year heat map and a cumulative distribution [5]. From Figure 2a, we can observe that low electricity prices occur during the solar day, while peak prices occur either in the morning or early evening hours. From Figure 2b, we can observe the distribution of electricity prices and that approximately 10% of the annual hours have a normalized price of less than 0.05. On the other end of the distribution, approximately 10% of the annual hours have a normalized price greater than 1.5.

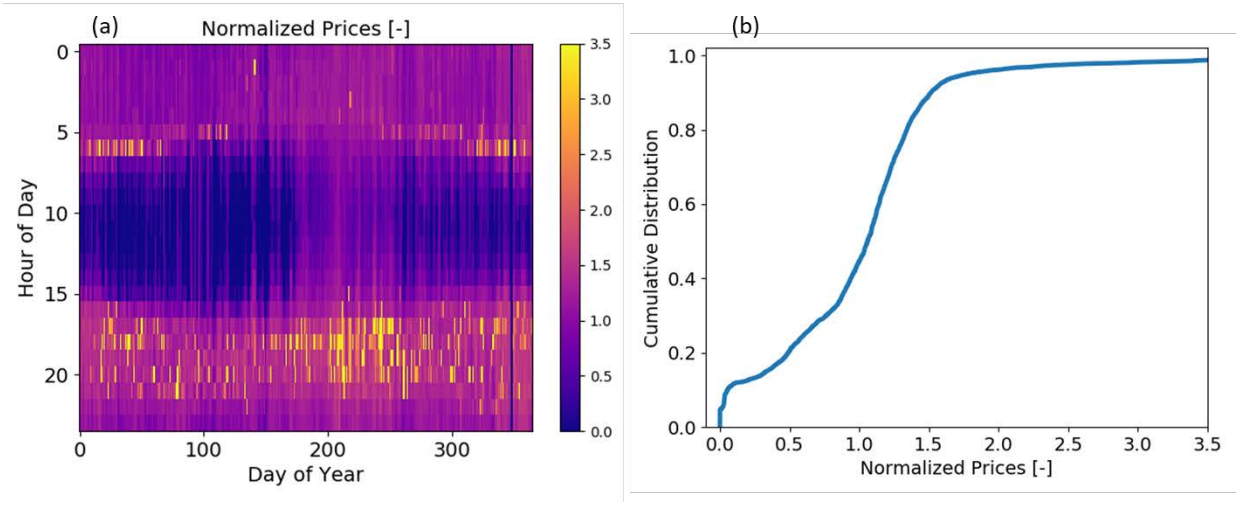

Figure 2. Normalized prices from the 2030 "Target high solar" California PLEXOS scenario as (a) a time of year heat map and (b) a cumulative distribution

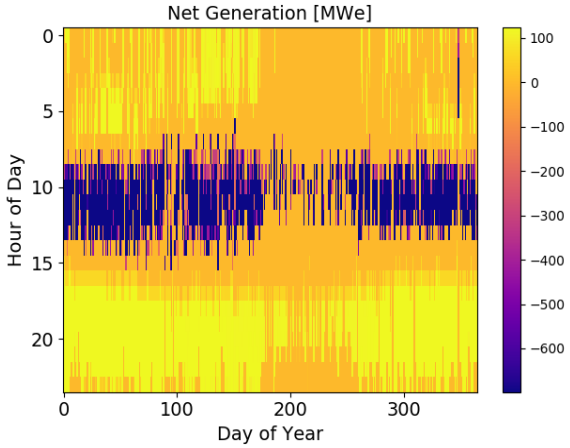

Figure 3. ETES net generation with 12 hours of storage and a heater multiple of 2.5 as a time of the year heat map

Figure 3 depicts the net generation throughout the year, using our developed SAM model with dispatch optimization for optimal ETES scheduling, of an ETES system with a fixed design of 12 hours of storage and a heater multiple of 2.5. From this figure, we can observe the charge (shown in purple) and discharge (shown in yellow) operations through the annual simulation. Charging occurs typically between the 9th (9 a.m.) and 13th (1 p.m.) hour of day. Discharging occurs in the early evening corresponding to the higher price periods presented in Figure 2a. Additionally, from Figure 3, we observe there is a seasonal variation in the ETES utilization. During the summer months, the ETES system's TES capacity is underutilized, shown as shorter charge and discharge periods. Figure 4 presents the daily low-to-high electricity price ratio throughout the year. From this, we can observe during summer months (i.e., 180 to 250 day of year) this ratio tends to be constantly higher than other times of the year. This result is specific to the price signal used in this analysis. However, this result shows the advantage of using dispatch

optimization over fixed block scheduling for simulation analysis, as the dispatch optimization model can dynamically make optimal operating decisions for the ETES system.

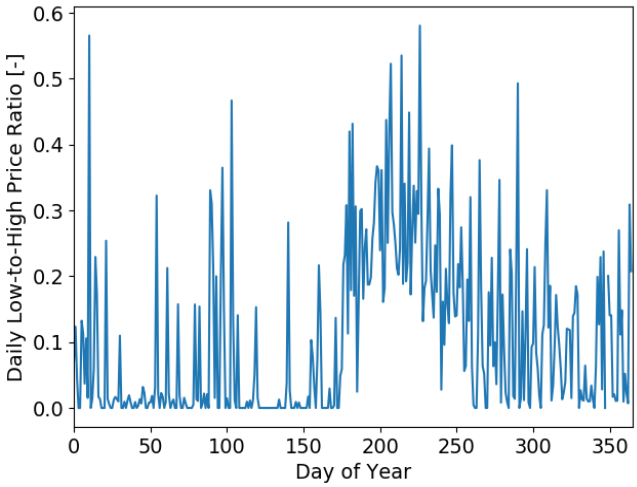

Figure 4. The daily ratio of minimum to maximum electricity prices throughout the year

Figure 5 presents ETES annual performance metrics for varying hours of storage and heater multiple. Annual performance metrics include: (1) annual gross profit assuming an average energy price of $75/MWh, (2) annual net generation (electricity out less electricity in), (3) generation to load ratio, and (4) TES utilization. In these figures, we have explicitly pointed the direction of increasing capital investment, i.e., high hours of storage and high heater multiple. From the parameter space we explored, a trade-off exists between ETES earning potential and capital investment (shown in Figure 5a). As hours of storage increases, annual gross profit also increases; however, there becomes a point where increasing the hours of storage has diminishing returns because the ETES system exploits all the profitable operating time periods throughout the year. This inflection point depends on the heater multiple as seen in Figure 5a.

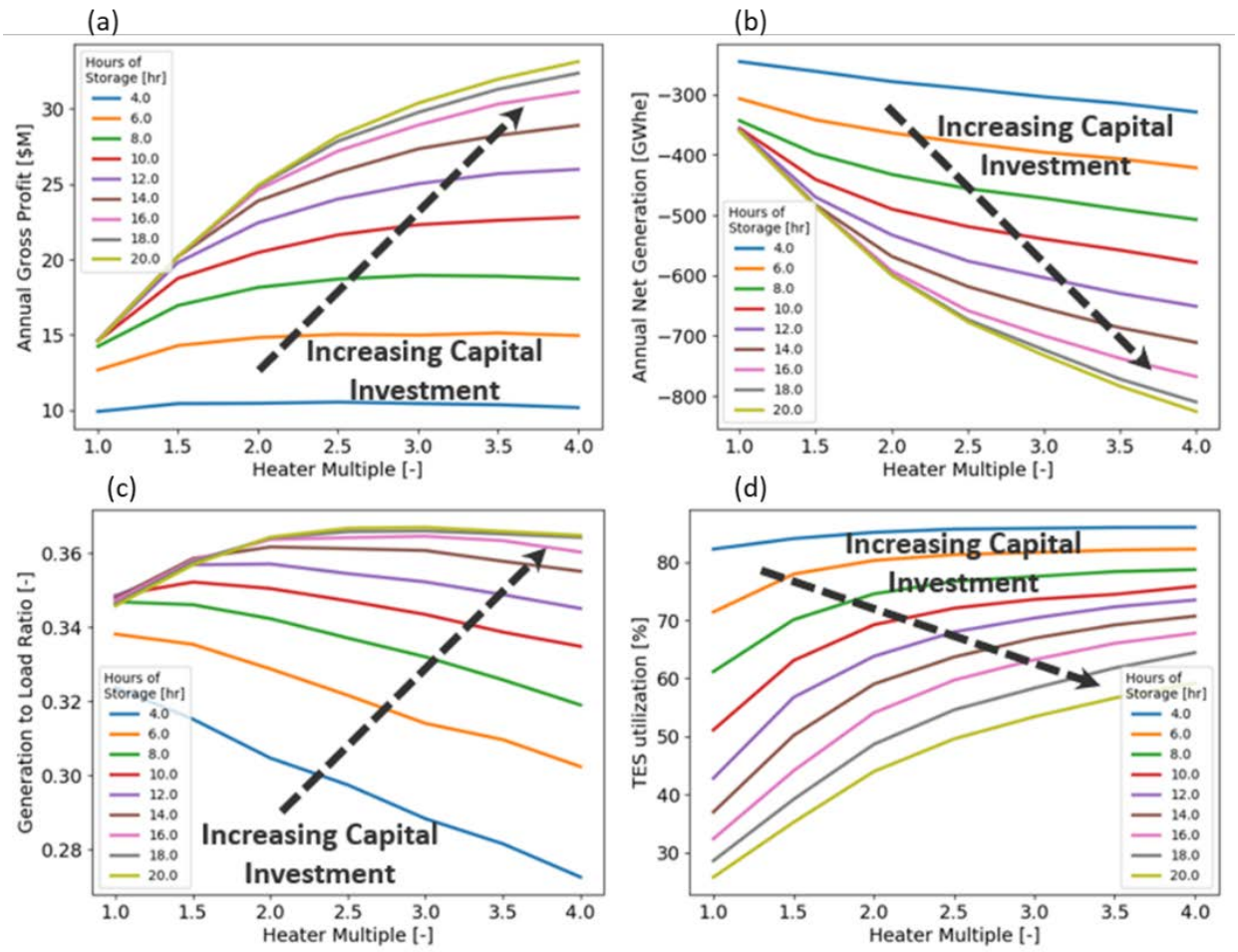

Figure 5. Full-factorial design of hours of storage and heater multiple annual performance metrics using dispatch optimization for optimal ETES scheduling. Annual performance metrics include: (a) annual gross profit assuming an average energy price of $75/MWh, (b) annual net generation, (c) generation to load ratio, and (d) TES utilization.

As the ETES system increases in size, the annual net generation decreases because the system operates for longer durations and thereby consumes more energy (shown in Figure 5b). The generation-to-load ratio represents the system's true round-trip efficiency over the course of a year. As the system operates longer due to increasing hours of storage, the ETES system reaches a limiting generation to load ratio depending on heater multiple (shown in Figure 5c). Lastly, TES utilization is defined as the average daily TES state-of-charge, which provides a sense of TES operations.

Figure 6 presents the internal rate of return (IRR), assuming an average annual energy price of $75/MWh, for each combination of hour of storage and heater multiple. We observe the

maximum IRR, approximately 13%,[1] occurs using 16 hours of storage and a heater multiple of 3.0. For all the hours of storage, we obverse a heater multiple that maximizes IRR of the ETES system. As hours of storage increase, the heater multiple that provides maximum system IRR also increases. The default values in SAM for inflation rate and real discount rate are 2.5%/year and 6.4%/year which result in a nominal discount rate of 9.06%/year. This means for any IRR greater than 9.06%, in Figure 6, the ETES system configuration will have a positive net present value.

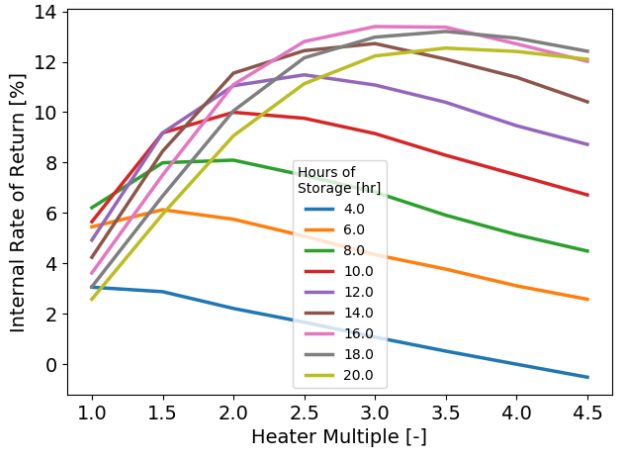

Figure 6. Internal rate of return for each configuration in the full-factorial design

3.3.3 ETES and CSP Dispatch Optimization Refactoring

To fully integrate the ETES dispatch optimization model into SAM, a major effort was required to refactor the ETES and CSP dispatch optimization models to enable sharing of core functionality needed by both code bases. This refactoring reduces the amount of repeated code within SAM's simulation core (SSC), which improves SSC's maintainability. Additionally, this code refactoring enables the SSC dispatch optimization method to be more modular, which improves code flexibility and enables the ability to apply this method to future modeled dispatchable technologies.

To complete this refactoring, we created a "base_dispatch" class that provides core structure that must be followed by the ETES and CSP dispatch child classes. This core structure includes: (1) solver parameters used by the dispatch solver LPsolve, (2) object pointers used by the dispatch class to get parameter values from the performance models and to communicate messages back to the user interface, (3) LPsolve outputs for reporting the quality of the solution to the users, and (4) dispatch solution outputs used to communicate the dispatch estimates and targets to the performance model. From this "base_dispatch" class, we can create child classes for ETES and CSP dispatch optimization models. These child classes house the specific technology parameters

[1] Note that the electricity pricing schedule used in this analysis is from a future grid scenario and that performance and cost inputs are borrowed from CSP model defaults and do not necessary represent realistic ETES values. The results here are useful to illustrate the dispatch model and resulting relationships between design parameters, but the absolute values of financial metrics like IRR carry significant uncertainty. Additionally, the assumed average annual energy price of $75/MWh is about double of "typical" average electricity pricing.

required to create the mixed integer linear program dispatch optimization model, the variable values determined by LPsolve, and the specific methods the simulation controller uses to interact with the dispatch classes.

We compared CSP model results with dispatch optimization before and after refactoring, which allowed us to catch any accidental errors introduced. After debugging, we were able to match the CSP model outputs exactly for the annual simulation metrics provided by SAM (i.e., annual energy, capacity factor, annual water usage, year 1 power purchase agreement (PPA) price, levelized PPA price nominal, levelized PPA price real, levelized cost of energy (LCOE) nominal, LCOE real, net present value, net capital cost, equity, and size of debt). While this effort did not (and was not expected to) change the model results, it was important work to enable future success of dispatch optimization modeling within SSC, including the ETES-CSP hybrid model for this project.

3.3.4 ETES Dispatch Optimization Model Absolute Grid Pricing and Solver Tuning

Next, we switched to providing the dispatch optimization model absolute grid prices in the form of dollars per energy instead of a normalized price signal, which has been historically used in the CSP dispatch model. We observed significant degradation in dispatch solution speed and quality due to more problem instances reaching the imposed solver time limit of five seconds. After internal group discussions, we felt the best method forward was to use absolute grid pricing for the following two reasons: (1) it provides consistent units for all terms within the objective function and (2) it allows the dispatch model to evaluate the direct comparison between potential revenue gain and cost of operating the system. The latter is a critical operational decision that we want to capture within this dispatch optimization model. Therefore, we must overcome the degraded dispatch solution times and improve problem tractability to enable the use of absolute grid prices.

We started addressing this issue by understanding how the problem structure changes when switching from normalized to absolute grid prices. Specifically, the input data changes by at least an order of magnitude from normalized prices centered around 1 to absolute prices with an expected maximum value of $0.2/kWh or $200/MWh. Additionally, the dispatch optimization problem variables were in the units of kilowatts, resulting in variable values on the order of 10^6. This range of magnitude between parameter and variable values can have a significant impact of problem structure and numerical stability of the solver. To overcome this obstacle, we scaled the dispatch problem to be in units of megawatts, which more closely aligns with the scale of the systems modeled in SAM.

The condition number of the constraint matrix is used in numerical analysis to understand the numerical stability of a linear program. In a sense, the smaller the condition number of the constraint matrix the more accurate solution can be provided by algorithms using said matrix. Before scaling the dispatch problem, we observed a condition number of about 2.8e-7 when using absolute prices which LPSolve considers marginal numeric accuracy. After scaling to megawatts, we observed a condition number of about 2.3e-10, which LPSolve considers “excellent” numeric accuracy. Additionally, we observed a reduction in the constraint matrix dynamic range by three orders of magnitude, specifically from 2.67e6 to 2.67e3.

Table 3. Annual Simulation Time, Number of Suboptimal Solutions, and Annual Revenue for the Kilowatt- and Megawatt-Scale Versions of the Dispatch Model

Additionally, we present results for the megawatt scale with a 60-second dispatch solve time limit. Note that this comparison reflects the state of the model directly after the conversion to the megawatt-scale model. Currently the default SAM case runs in 217 seconds.

	Simulation Time [seconds]	Suboptimal Solutions [-]	Annual Revenue [$M]
Kilowatt Scale	2001.3	269	12.938
Megawatt Scale	897.3	60	14.629
Relative Difference [%]	-55.2	-77.7	13.1
Megawatt Scale (60 Second Timeout)	1637.5	2	14.694

A comparison of simulation time, number of suboptimal solutions, and annual revenue for the kilowatt- and megawatt-scale versions of the dispatch model is presented in Table 3. For an annual simulation, we solve 365 dispatch problems, each with a 48-hour look-ahead horizon. By scaling the dispatch model from kilowatts to megawatts, we observe significant improvements in solution time and solution quality in the form of annual revenue. During the annual simulation using the kilowatt-scale dispatch model, we observed 47 instances where the initial dispatch model failed due to numerical scaling issues, resulting in the solver rescaling the problem to improve problem numerical stability and converge to a solution. For the megawatt-scale dispatch model results, there were 60 suboptimal solutions that were a result of reaching the default dispatch solution time limit of 5 seconds. We resolved the megawatt-scale model using a 60-second time limit to understand the potential revenue lost by these suboptimal solutions. From Table 3, we observe a 0.4% increase in annual revenue, or about $65k, when using the 60-second time limit. However, we see an 82% increase in annual simulation time. Figure 7 (right) presents the relative difference in objective value between the 60- and 5-second time limit solves when the 5-second solve limit was reached. We observe that the majority of 5-second timeout objectives are within 2.5% of the objectives found by the 60-second timeout limit.

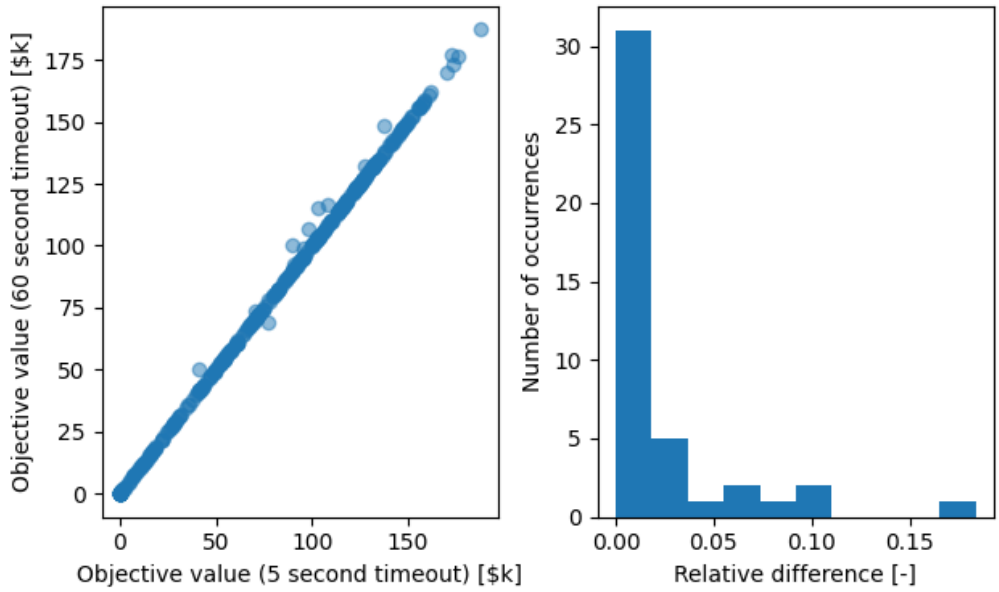

Figure 7. Direct comparison between the objective function value using a 60-second time limit and the default 5-second time limit (left), and the relative difference in objective value between the 60- and 5-second time limit solves (right)

3.4 Molten Salt Power Tower—ETES Hybrid Model

We also added the capability to model an ETES-CSP MSPT hybrid plant. The hybrid model adds the resistive heater in parallel to the MSPT, such that the heater receives cold HTF from the cold TES tank, heats it to a target outlet temperature, and then delivers the hot HTF to the hot TES tank. Implementation of the resistive heater model as a "parallel heat source" in SAM's modeling framework requires modification to the resistive heater, plant convergence, and plant controller models as follows:

- The CSP plant controller models the startup time of the receiver rather than just deducting startup energy from normal operations. This allows the model to realistically sequence plant operations as solar resource becomes available. This feature is one of the most complicated pieces of the plant numerical convergence code, because (1) it requires iterating on timestep duration and (2) the receiver and cycle can simultaneously startup. As such, adding another component startup procedure to the timestep iteration would add substantial complexity to both the numerical convergence routines and the plant controller. As such, we decided, for the hybrid case only, to model resistive heater startup as an instantaneous process that incurs an electric parasitic that is applied independently of the heater timestep operation. For example, if the plant controller wants the heater to turn on and operate at full load at noon, the model will run the heater at full load the entire timestep, but the electricity consumption will be larger to account for the startup energy. We think this simplification is more reasonable for the heater than a solar receiver because the startup time requirement should be shorter. Furthermore, unlike solar resource, electricity is always available to startup the heater, so we can assume the startup could have happened at the end of the previous timestep.

- We added the resistive heater class as a second "solar field" class in the system model. Then we added a separate control signal for the heater that the plant controller sets. Finally, the

numerical convergence model solves both the solar receiver and heater performance and performs a mass balance and enthalpy mix on their outputs to send to the TES.

We added plant controller logic to include operating modes where the heater is on (when the heater is off, the required operating modes are captured by the existing model). The logic ensures that the heater can't operate if the cycle is generating electricity. The controller also applies sequenced defocus in cases where both the receiver and the heater are operating, and the plant cannot use the total heat. First, the controller will defocus the heater. If the total output from the receiver and fully defocused heater still provides too much heat, then the controller will turn off the heater and defocus the receiver as necessary.

- Appendix A: Hybrid ETES-MSPT Plant Controller Diagrams includes logic diagrams for the controller, with each diagram corresponding to a different combination of component initial conditions.

The hybrid plant dispatch model combines the MSPT and ETES dispatch component models, and it uses the common objective to maximize revenue. Figure 8 shows timeseries results of the model for a plant design that adds a heater at a heater multiple of 2 to the default MSPT case with a solar multiple of 2.4 and 10 hours of storage. The first day has good solar resource, so the plant only operates the heater near full load for one hour and at part load for another hour when the electricity price multiplier is low. Dispatch instructs the plant to turn on the cycle in the early afternoon so that the receiver does not need to defocus. The second day has poor solar resource, and the plant never operates the receiver. Instead, dispatch operates during low-cost-electricity periods to fill storage. For both days, the plant discharges storage when electricity prices are relatively high.

3.5 Comparison of ETES Operation and Revenue Between SAM and PLEXOS

Here we seek to validate the SAM ETES dispatch optimization model by comparing annual operational schedules and annual revenue against that obtained from simulating the same ETES system in PLEXOS, which is a unit commitment model. The SAM ETES model is a price-taker model, which aims to maximize revenue for the ETES system given constraints on ETES operation and a known, fixed, time-series price signal. PLEXOS, on the other hand, is a production cost model that simultaneously co-optimizes operations of *all generators* in the simulated grid to minimize the cost of satisfying electricity demand and ancillary services requirements subject to transmission constraints and operational constraints for each generator. The implementation of the ETES system in PLEXOS was adapted from models developed previously for pumped thermal energy storage (PTES) systems in PLEXOS [6]. The SAM ETES model can include more complexity in ETES system behavior than can be included in the PLEXOS implementation, and thus we adapted input parameters in SAM to match the description of the ETES system in PLEXOS as shown in Table 4. In addition, a user-defined power cycle in SAM was defined to match the part-load and ambient temperature characteristics captured in the PLEXOS implementation.

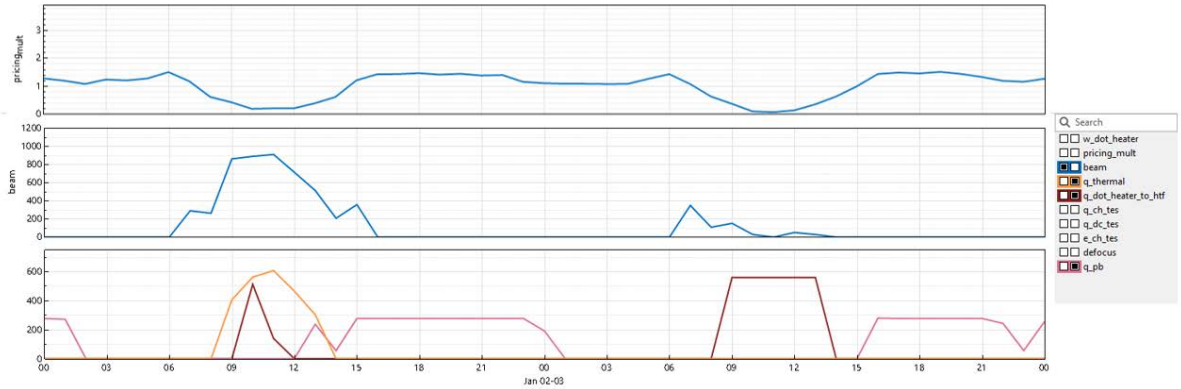

Figure 8. Example of ETES-MSPT hybrid performance and dispatch model results

The plant design adds a heater at a heater multiple of 2 to the default MSPT case with a solar multiple of 2.4 and 10 hours of storage.

Table 4. Input Parameters for Comparison of SAM and PLEXOS ETES Models

Parameter	Value	Parameter	Value
Cycle gross capacity (MWe)	100 (SAM), 100-1000 (PLEXOS)	Heater startup time/energy requirement	None
TES capacity	10 hours	Parasitic loads	0
Heater multiple	2	Cycle start cost	$42/MWe
Design point cycle efficiency	0.395	Heater start cost	$10/MWe
Min/Max cycle or heater load fraction	0.25 / 1.0	Cycle ramping cost	$0
Cycle startup energy requirement	20% of cycle capacity	Variable O&M cost	$1.1/MWhe
Cycle startup time requirement	None	Outage rate	0%

We first simulated a base case grid scenario in PLEXOS without the ETES system and extracted hourly locational marginal electricity prices (LMPs) at a designated node in the model. These base case electricity prices provided the hourly price signal against which the SAM ETES plant was dispatched. The PLEXOS model was then reevaluated after adding an ETES system at the same location. Table 5 provides two separate pre-existing grid scenarios used for the analysis. The first is a hypothetical representation of the U.S. Western Interconnection in 2030, guided by states' renewable portfolio standards circa ~2016 under which 50% of electricity in California could be derived from renewable resources [5]. The second is a hypothetical representation of the Texas Interconnection with 33% wind penetration.

Table 5. Grid Scenarios

	LCGS Target High Solar [5]	**ERCOT Mid Wind** [7]
Full model geographical area	Western Interconnection	Texas Interconnection
ETES plant location	Ivanpah, CA	Van Horn, TX
Annual photovoltaic (PV) contribution [a]	10.5% (38.2%)	0.3% (0.2%)

	LCGS Target High Solar [5]	ERCOT Mid Wind [7]
Annual wind contribution [a]	10.5% (16%)	33.7% (86.7%)
Annual PV curtailment (GWh)[a]	2665 (609)	5 (1)
Annual wind curtailment (GWh)[a]	567 (95)	4956 (1974)

[a] Model-wide (region containing Ivanpah, CA or Van Horn, TX)

Figure 9, Figure 10, and Figure 11 illustrate hourly heat maps of the base case LMP at the ETES plant location, the PLEXOS ETES cycle and heater load fractions, and the hourly difference between SAM and PLEXOS solutions in the low-carbon grid scenario (LCGS) scenario. In this PV-dominated scenario ETES charging typically occurs midday using curtailed or low-cost PV electricity, while discharging occurs in the evening and early morning.

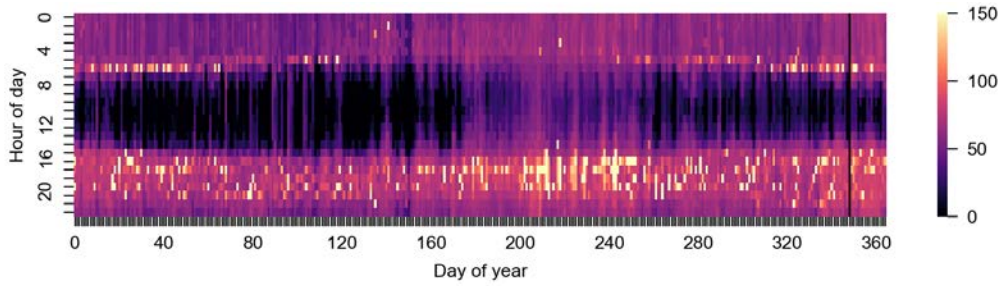

Figure 9. Electricity price at the selected location from the base case PLEXOS model of the LCGS scenario

Note that the color scale is saturated at the upper bound to better show differences in price.

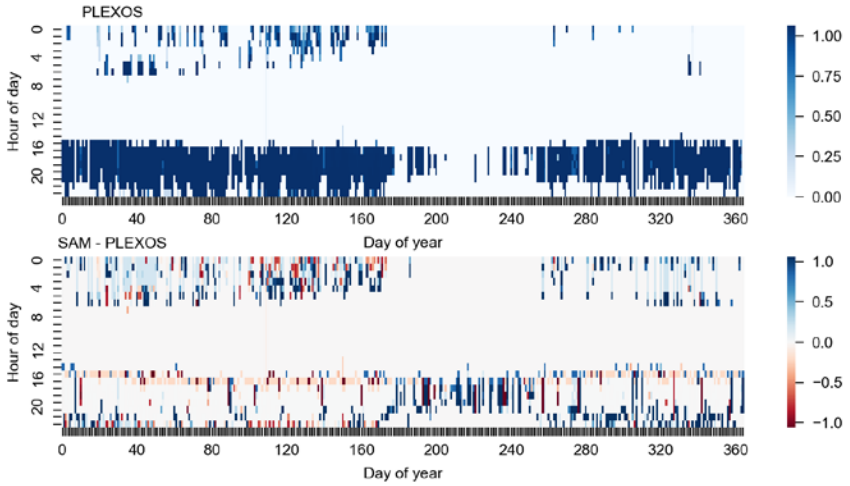

Figure 10. Power cycle load fraction in the LCGS scenario (500 MWe ETES)

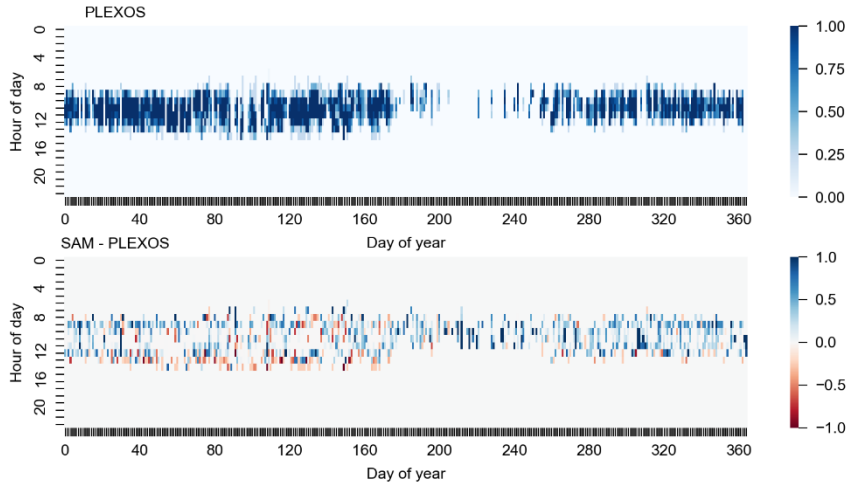

Figure 11. Heater load fraction in the LCGS scenario (500 MWe ETES)

SAM and PLEXOS produce generally similar operational patterns, with many of the differences occurring in the first/last hours of the charging or discharging cycles. For the power cycle, this is in part due to slight differences in how PLEXOS and SAM incorporate startup energy loss. In addition, the SAM ETES solution tends to more aggressively chase price peaks in the morning hours (and operate at part load overnight to avoid an additional startup/shutdown cycle), and it operates more frequently in the summer.

Table 6 provides the total annual electricity generation, heater load, number of starts, and gross/net revenue for the LCGS scenario at three different simulated ETES plant capacities in PLEXOS. Here the gross revenue is the sum of the LMP multiplied by the net electricity generation (cycle generation minus heater load), while net revenue is simply gross revenue less start costs and variable O&M costs. Table 7 provides the relative differences in revenue calculated using (1) base case LMP for both SAM and PLEXOS solutions, and (2) base case LMP for the SAM solution and LMP after ETES addition for the PLEXOS solution.

Table 6. Annual Operation and Revenue for the LCGS Scenario

	SAM	PLEXOS		
Simulated cycle gross capacity (MWe)	100	1,000	500	250
Cycle electricity generation (MWhe/MWe heat engine capacity)	2,568	1,814	2,094	2,268
Heater load (MWhe/MWe heat engine capacity)	6,448	4,554	5,256	5,688
Annual cycle starts	327	297	332	361
Annual heater starts	311	273	289	304
Value and revenue ($M / GWe cycle capacity)				
PLEXOS ETES value		49.3	67.2	65.1
Gross revenue (base case prices)	153	123	135	141
Net revenue (base case prices)	126	100	110	114
Gross revenue (prices after ETES)		62	95	118
Net revenue (prices after ETES		40	70	91

Table 7. Difference Between SAM and PLEXOS Solution for Gross (Net) Revenue

Positive values indicate higher revenue from SAM than PLEXOS.

	LCGS		
PLEXOS gross cycle capacity (MWe)	1000	500	250
Both using base case LMP	25% (26%)	13% (14%)	8% (10%)
PLEXOS using LMP after ETES	146% (216%)	61% (80%)	29% (38%)

SAM and PLEXOS revenue differ by less than 15% for all except the highest capacity simulated in PLEXOS when revenue is calculated using base case LMP. This is the only set of prices known to the SAM model, but it is not the most realistic representation of revenue available from PLEXOS. The operation of the ETES system within PLEXOS can completely offset the highest marginal cost generators in some hours and use up all locally available curtailed or low-cost electricity in other hours, thereby decreasing the LMP in high-price hours and increasing the LMP in low-price hours. This price suppression/elevation is negligible for a marginal ETES capacity but can become significant at large ETES capacities and can be seen in Table 6 in the reduction in revenue from the PLEXOS solution when using LMP after the addition of the ETES system. Thus, for a non-marginal capacity generator, the SAM price-taker solution can be expected to produce an estimate of revenue that is too high; however, the magnitude of this overestimation is strongly tied to the grid scenario and plant capacity. The smallest ETES system capacity than can be meaningfully simulated in PLEXOS must produce changes in total systemwide production cost substantially above the optimization mip gap tolerance. Here we use a mip gap of 0.075%, and the total change in production cost for the lowest simulated ETES capacity (250 MWe) approaches this tolerance. Thus, we cannot obtain a meaningful estimate for a realistic single 100-MWe plant capacity in this scenario. Furthermore, while SAM and PLEXOS solutions can be expected to match most closely at a small plant capacity, the larger plant capacities in PLEXOS can be expected to have better resolution in the optimal solutions.

The fact that differences exist between SAM and PLEXOS solutions is not necessarily indicative of problems in the SAM price-taker model formulation, but instead likely indicates general challenges of using price-taker model formulations for storage systems. In addition to the price-suppression/elevation issue described above, SAM's price-taker model uses LMPs from PLEXOS that capture instantaneous marginal generation costs (fuel usage, variable O&M, emissions costs) but do not include start costs from other generators. The ETES system in this PLEXOS scenario derives approximately 30%–40% of its total value (the decrease in total systemwide production costs upon addition of the ETES system to the grid) from avoided start costs of other generators, which can only be captured in the optimal solution from a price-taker model indirectly if the timing of operations to avoid these start costs happens to coincide with the timing required to maximize ETES revenue. It is also possible that shallow optima and imperfect solution tolerance are contributing to the observed differences.

Figure 12, Figure 13, Figure 14, Table 8, and Table 9 provide analogous results for the ERCOT scenario. Unlike the LCGS scenario, the wind-dominated ERCOT scenario exhibits wind curtailment and low prices overnight, with peak prices occurring midday and generally lower peak prices. As in the LCGS scenario, the ETES system dispatched by SAM system tends to operate more frequently than that dispatched by PLEXOS; however, the differences in annual electricity generation and heater electrical load are less than 5% for simulated 250-MWe and 100-MWe ETES power cycle capacities. The calculated gross or net revenue for the ETES system using the optimal dispatch schedule from SAM exceeds that from PLEXOS, with the magnitude of this difference decreasing to approximately 10% at the smallest simulated plant capacity (100 MWe). The ERCOT scenario is significantly smaller than the LCGS scenario, and here a 100-MWe ETES plant capacity can be simulated in PLEXOS with an overall change in systemwide production cost of 0.12%, slightly above the mip gap tolerance of 0.075%. As in the LCGS scenario, SAM has the potential to significantly overestimate revenue when changes in price resulting from the operation of the ETES system are taken into account (bottom row of Table 6). The magnitude of this difference decreases significantly with simulated plant capacity and, at a 100-MWe capacity, was only 13%.

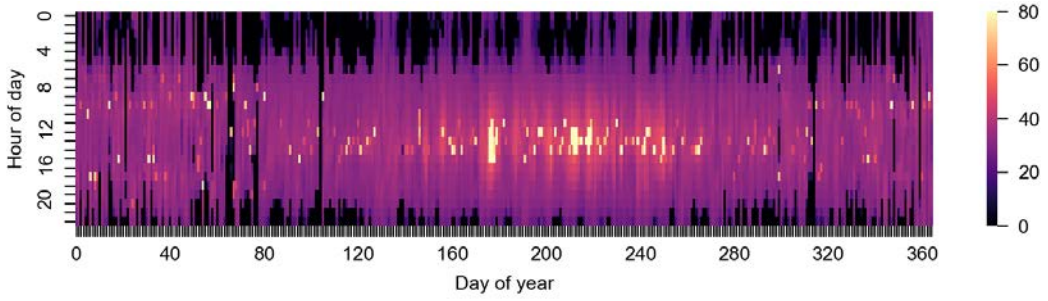

Figure 12 Electricity price at the selected location from the base case PLEXOS model of the ERCOT scenario

Note that the color scale is saturated at the upper bound to better show differences in price.

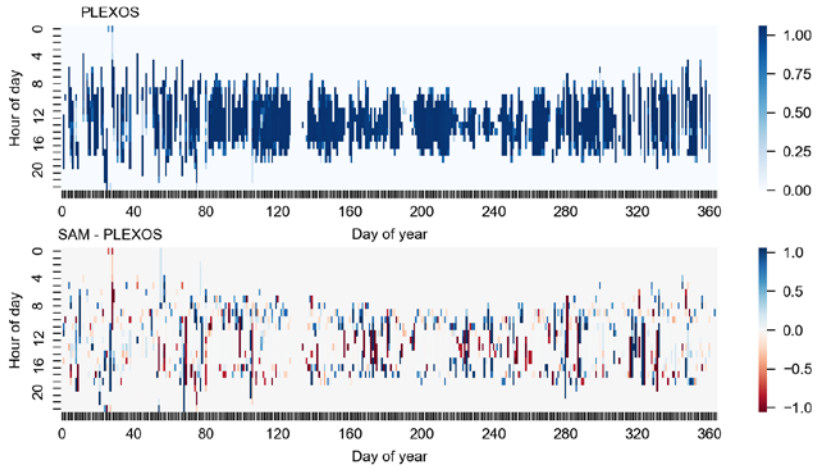

Figure 13. Power cycle load fraction in the ERCOT scenario (250 MWe ETES)

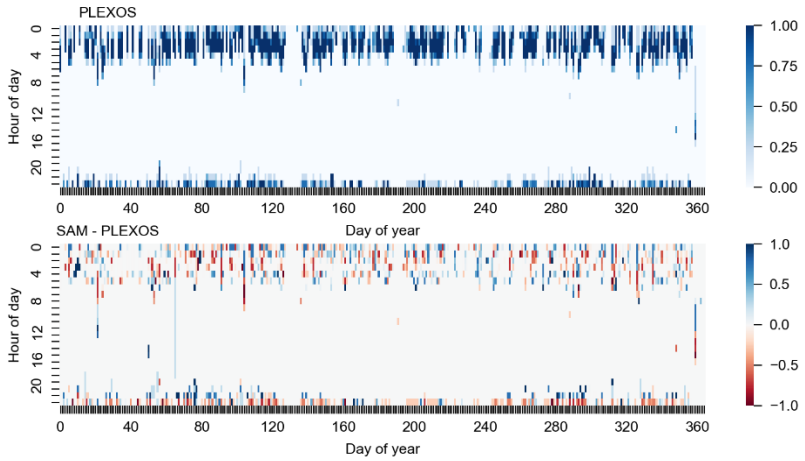

Figure 14. Heater load fraction in the ERCOT scenario (250 MWe ETES)

Table 8. Annual Operation and Revenue for the ERCOT Scenario

	SAM	PLEXOS		
Simulated cycle gross capacity (MWe)	100	500	250	100
Cycle electricity generation (MWhe/MWe heat engine capacity)	2,305	2,058	2,199	2,249
Heater load (MWhe/MWe heat engine capacity)	5,764	5,214	5,557	5,685
Annual cycle starts	260	291	296	298
Annual heater starts	252	271	286	290
Value and revenue ($M / GWe cycle capacity)				
PLEXOS ETES value		58.2	68.9	70.4
Gross revenue (base case prices)	92	82	86	88
Net revenue (base case prices)	70	59	62	64
Gross revenue (prices after ETES)		66	79	86
Net revenue (prices after ETES		43	55	62

Table 9. Difference Between SAM and PLEXOS Solution for Gross (Net) Revenue

Positive values indicate higher revenue from SAM than PLEXOS.

	ERCOT		
PLEXOS gross cycle capacity (MWe)	500	250	100
Both with base case prices	13% (19%)	7% (12%)	5% (9%)
PLEXOS with prices after ETES	40% (63%)	17% (26%)	8% (13%)

3.6 Comparison of Hybrid ETES-MSPT Operation and Revenue Between SAM and PLEXOS

We also compared solutions from the SAM dispatch optimization model for a hybrid CSP-ETES system against those obtained from simulating the same CSP-ETES system in PLEXOS. The CSP-ETES plant is in Ivanpah, CA. Table 10 contains properties describing the CSP-ETES system in both SAM and PLEXOS models and was adopted from previously solved models for a PTES, CSP-PTES, and CSP-ETES in PLEXOS [6]. Remaining parameters were set to SAM default values. The SAM CSP-ETES model can include more complexity in system behavior than can be included in the PLEXOS implementation, and thus we adapted input parameters in SAM to match the description of the CSP-ETES system in PLEXOS as shown in Table 10. A user-defined power cycle in SAM was used to match the part-load and ambient temperature characteristics captured in the PLEXOS implementation. The PLEXOS model does not directly simulate the CSP field receiver, and instead takes as input the hourly thermal energy generation in the field/receiver simulated in SAM.

As for the stand-alone ETES system, note that the large CSP-ETES capacity simulated in the PLEXOS model is driven by the capacity required to produce changes in total systemwide production cost (the objective function for the PLEXOS model) that are outside of the imperfect optimization tolerance for the large-scale simulated grid.

Table 10. Input Parameters for Comparison of SAM and PLEXOS

Parameter	Value	Parameter	Value
Cycle gross capacity (MWe)	100 (SAM), 1000 (PLEXOS)	Heater startup time requirement	None
CSP solar multiple (SM)	1.0 (Case 1) 2.0 (Case 2)	Cycle start cost	$42/MWe
TES capacity	10 hours (Case 1) 14 hours (Case 2)	Heater start cost	$10/MWe
Heater multiple	1.0	Cycle ramping cost	$0
Design point cycle efficiency	0.395	Variable O&M cost	$1.1/MWhe
Min/Max cycle or heater load fraction	0.25 / 1.0	Outage rate	0%
Cycle startup energy requirement	20% of cycle capacity	Simultaneously operation of cycle and heater allowed?	Yes (PLEXOS) No (SAM)
Cycle startup time requirement	None	-	-

Figure 15, Figure 16, Figure 17, and Figure 18 illustrate hourly heat maps of the PLEXOS solutions for CSP-ETES cycle and heater load fractions, and the hourly difference between SAM and PLEXOS solutions. As in the stand-alone ETES results, SAM and PLEXOS solutions generally show similar daily and seasonal usage patterns with hour-by-hour differences primarily occurring at the beginning/end of charge or discharge time blocks. This is likely partially due to small discrepancies in how each model handles component startup, but it is also likely a result of shallow optima with a multitude of solutions producing systemwide production cost (PLEXOS) or CSP-ETES revenue (SAM) that can't be distinguished within the optimization tolerance. In each case the electric heater operates predominantly during a similar timeframe as CSP thermal generation, as the time periods with the lowest prices are those with substantial solar resource in this PV-dominated grid scenario. Correspondingly, the electric heater utilization is lower in the case with a higher CSP solar multiple because of limited thermal storage reserves.

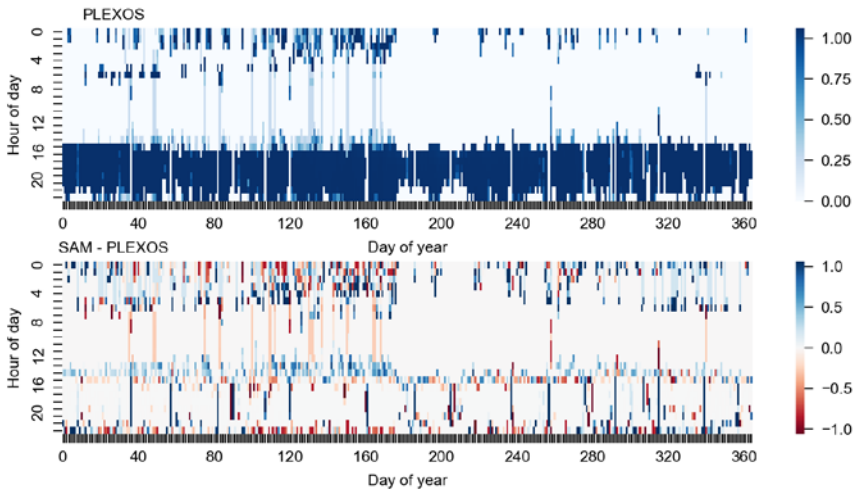

Figure 15. Power cycle load fraction with SM = 1, TES = 10 hours

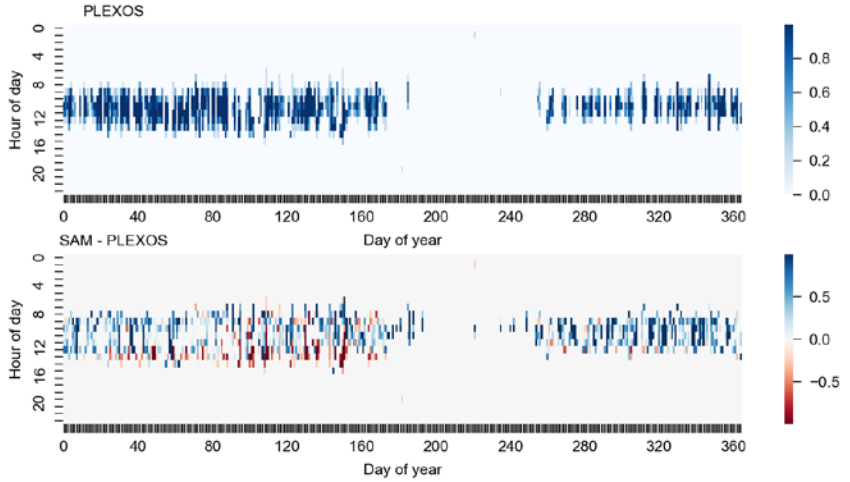

Figure 16. Electric heater load fraction with SM = 1, TES = 10 hours

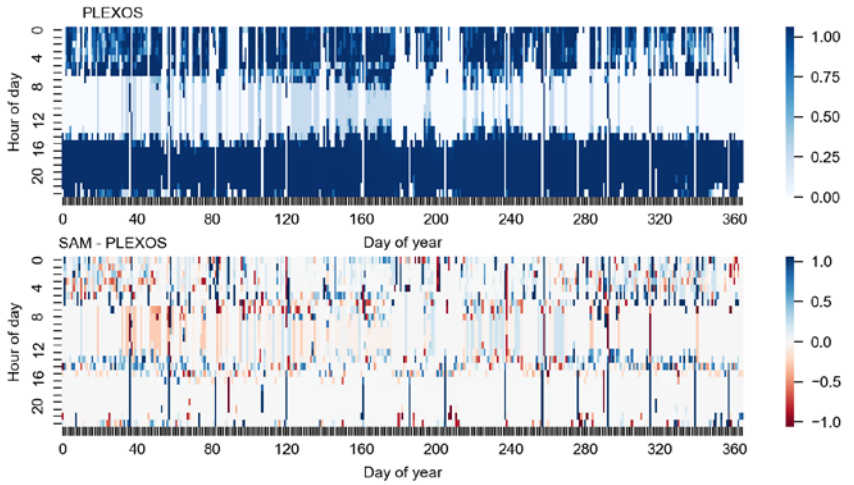

Figure 17. Power cycle load fraction with SM = 2, TES = 14 hours

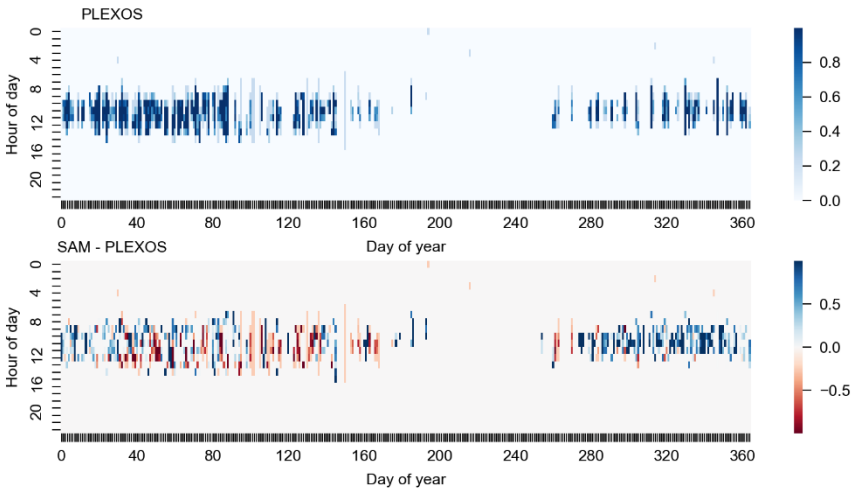

Figure 18. Electric heater load fraction with SM = 2, TES = 14 hours

Table 11 provides the total annual electricity generation, heater load, number of starts, and gross/net revenue. Here the gross revenue is the sum of the LMP multiplied by the net electricity generation (cycle net generation minus heater load), while net revenue is simply gross revenue less start costs and variable O&M costs. Table 12 provides the relative differences in revenue calculated using (1) base case LMP for both SAM and PLEXOS solutions, and (2) base case LMP for the SAM solution and LMP after CSP-ETES addition in the PLEXOS solution.

When compared using a consistent price signal (top row of Table 12), the SAM and PLEXOS revenue differs by less than 4.5% in each simulated case. This suggests that the operational differences that exist in

Table 11 and the figures above are relatively insignificant from the standpoint of revenue. As noted in the discussion of the stand-alone ETES case, the PLEXOS model captures interactions between CSP-ETES dispatch and operation of all other generations, and thus the LMP can decrease in hours when the CSP-ETES system is generating electricity and increase in hours when the CSP-ETES system is charging thermal storage using grid electricity. This price suppression/elevation implies that, for a non-marginal capacity generator, the SAM price-taker solution can be expected to overestimate revenue as is shown in the second row of Table 12. However, note that the magnitude of this overestimation is a strong function of the simulated capacity, and the large capacity (1,000 MWe) simulated in the PLEXOS model is a worst-case scenario compared to a more realistically sized single 100-MWe system. Revenue implications of price suppression/elevation appear to be substantially less significant in the CSP-ETES cases here than in the stand-alone ETES cases. This is because the discrepancies in the stand-alone ETES case came disproportionately from price elevation during charging. In the CSP-ETES cases the electric heater capacity is smaller, and the heater operates less frequently than the standalone ETES case. The differences between SAM and PLEXOS CSP-ETES net revenue are slightly higher, but generally similar in magnitude, to differences previously noted for CSP-only systems within the same grid model [8].

Table 11. Annual Operation and Revenue

	SM = 1, TES = 10		SM = 2, TES = 14	
	SAM	**PLEXOS**	**SAM**	**PLEXOS**
Simulated cycle capacity (MWe)	100	1,000	100	1,000
Cycle electricity generation (MWhe/MWe heat engine capacity)	3,279	2,988	5,213	5,032
Heater load (MWhe/MWe heat engine capacity)	2,841	1,943	1,907	1,330
Receiver + heater thermal generation (MWht/MWe heat engine capacity)	8,242	7,524	12,868	12,546
Annual heat engine starts	370	372	288	267
Annual heater starts	275	219	199	175
Annual receiver starts	424	440	416	446
Value and revenue ($M / GWe cycle capacity)				
PLEXOS CSP-ETES value	-	174.4	-	295.8
Gross revenue (base case prices)	235	225	350	341
Net revenue (base case prices)	210	202	328	321
Gross revenue (prices after CSP-ETES)	-	200	-	314
Net revenue (prices after CSP-ETES)	-	176	-	294

Table 12. Difference Between SAM and PLEXOS Solutions for Gross (Net) Revenue

Positive values indicate higher revenue from SAM than PLEXOS.

	SM = 1, TES = 10	SM = 2, TES = 10
Both using base case LMP	4.4% (4.0%)	2.5% (2.1%)
PLEXOS using LMP after CSP-ETES	19.0% (17.7%)	11.6% (11.5%)

3.7 Summary of PLEXOS Comparisons

The previous sections describe how a price-taker model such as SAM does not capture price elevation or suppression effects caused by the dispatchable generator, unlike a unit commitment model like PLEXOS. However, it is worth a brief discussion on the value of price-taker models. They are useful to analyze a particular ETES technology because they provide more detailed system and component models, solve orders-of-magnitude faster, and are available (in this case) as free open-source software. The model results represent the most optimistic returns considering grid arbitrage from the input electricity pricing. In turn, these results serve as a feasibility stage-gate: if the financial results (including potential capacity payments and payments for other services) do not show acceptable return, then a unit commitment model likely is not worth exploring. In contrast, if the price-taker model shows that returns are within an acceptable range, then an optimal configuration from the price-taker model is a good candidate for a reduced number of analyses in a unit commitment model that can show how the existence of the proposed technology on the grid can potentially change the electricity pricing.

3.8 PTES Model

Pumped thermal energy storage systems employ a heat pump to charge the hot tank in the hot TES and cold tank in the cold TES.[2] During discharge, a power cycle consumes heat from the hot tank in the hot TES (returning the storage fluid to the cold tank) and is cooled by the cold tank in the cold TES (returning the storage fluid to the hot tank). PTES systems require both hot and cold side TES to operate, so it is important that charge and discharge cycles are balanced such that hot and cold side TES have the same normalized charge/discharge capacity. If the hot and cold side TES were unbalanced, then there could be a scenario where the hot tank in the hot TES had storage fluid, but the cold tank in the cold TES was exhausted. In that case, the hot TES would either be unusable, or the power cycle would have to operate at severe off-design because the cycle would not be able to cool its working fluid to the design cold temperature. The round-trip efficiency of the PTES system is less than 100% due to turbomachinery inefficiencies and heat exchanger approach temperatures, so the balance between electricity consumed during charging and the electricity generated during discharge must leave the system as heat. For a given heat transfer on the hot side, the power cycle rejects more heat on the cold side than the heat pump absorbs. As such, the system design and off-design operation must simultaneously balance hot side and cold side TES while rejecting waste heat to the environment and maximizing efficiency.

There are many combinations of working fluids, cycle configurations, and TES technologies possible to design a PTES system. Several distinct technologies are being commercialized, including air-Brayton cycles with two-tank TES and trans-critical CO_2 with hot side two-tank TES and cold-side phase change TES. Within a given cycle configuration, there is usually an option to replace cycle recuperation with TES that spans the entire temperature differential between the compressor outlet and turbine inlet. This typically requires a stable TES over a large temperature range, so particle TES is often proposed for these scenarios.

[2] While TES technologies like thermoclines or phase change storage are proposed for various PTES designs, we assume two-tank TES in the following discussion.

Given the wide variety of possible PTES system designs and the constraints imposed by balancing hot and cold side TES and rejecting waste heat, we developed a generalized framework for our nominal PTES system model. This framework allows users to specify high-level component information like cycle efficiency, heat pump coefficient of performance (COP), heat multiple, and TES temperatures. The heat pump and cycle component models apply simple scaling relationships to estimate the influence of TES temperatures and part-load. The system model converges mass and energy between the components and incorporates plant control and dispatch.

3.8.1 PTES System Design-Point

The PTES system design-point must consider the interdependencies between the cycle and heat-pump, because the heat pump requires knowledge of the cycle design heat input, and the cycle heat rejection split between cold TES and ambient requires knowledge of the heat pump COP. First, we calculate the high-level cycle design-point outputs using design parameters as shown in Table 13.

Table 13. Overview of Cycle Design Calculations for System Design

Design Parameter (Input)	Calculated Design Point (output)
Thermodynamic power output	Heat input
Thermodynamic efficiency	Thermodynamic power out
	Heat out (to both cold TES and ambient)

Next, we calculate the high-level heat pump design-point outputs using design parameters and constraints from the calculated cycle design-point as shown in Table 14.

Table 14. Overview of Heat Pump Design Calculations for System Design

Design Parameter (Input)	Constraint from Cycle Design	Calculated Design Point (output)
Thermodynamic COP of heat	Heat output (cycle heat input)	Heat in (cooling)
Heater multiple	-	Thermodynamic power in

Then, we use the ratio of heat pump heat in to heat out to calculate heat transferred from the cycle to the cold TES:

$$\dot{q}_{cycle\ to\ cold\ TES} = \dot{q}_{cycle\ in} \frac{\dot{q}_{heat\ pump\ cold\ in}}{\dot{q}_{heat\ pump\ hot\ out}} \quad (1)$$

Finally, the cycle design heat rejected to ambient is the difference between the total cycle design heat output and the design heat to cold TES.

3.8.2 PTES Power Cycle Design-Point and Off-Design Models

Using the system design-point described above, we use additional design parameters to fully define the cycle design-point as shown in Table 15. We call the entire design model from the user interface (UI) whenever an input changes. This allows the UI to instantaneously report the design-point parasitics and pumping power associated with a particular design. As such, the UI displays an accurate calculation of net system power associated with a given set of design parameters.

Table 15. Overview of Full Cycle Design Calculations

Design Parameter (Input)	Calculated Design Point (output)
Heat to cold TES (from System Design calcs)	Heat input
Thermodynamic power output	Thermodynamic power out
Thermodynamic efficiency	Total heat out
Electric parasitics as fraction of thermodynamic power	Net electric power out
Hot and cold TES cold and hot tank temperatures	Hot and cold HTF mass flow rates
Hot and cold HTF properties	Hot and cold HTF pumping power
Hot and cold HTF pumping power coefficients (kWe/kg/s)	Endoreversible efficiency

The cycle design model also calculates the design-point endoreversible efficiency based on the temperatures of the hot and cold TES as shown in Equation (2). We use this design value to estimate the influence of off-design TES temperatures on cycle efficiency.

$$\eta_{endoreversible} = 1.0 - \sqrt{\frac{0.5\left(T_{cold;cold\ TES} + T_{hot;cold\ TES}\right)}{0.5\left(T_{cold;hot\ TES} + T_{hot;hot\ TES}\right)}} \qquad (2)$$

We model the cycle off-design performance as a function of hot TES hot temperature, hot HTF mass flow rate, and cold TES cold temperature. The cycle model constrains the cycle such that the hot TES cold temperature and cold TES hot temperature return to their respective TES at their respective design temperatures. Given these inputs and constraints, summarized in Table 16, cycle performance is calculated as follows:

1. Calculate the heat input from inputs and constraints
2. Scale design efficiency by the product of:
    a. Ratio of off-design to design-point endoreversible efficiency

b. Part-load non-dimensional adjustment shown in Equation (3). This equation is only an approximation based on our cycle modeling experience that slowly decreases efficiency as the heat input moves away from design.

3. Use calculated off-design efficiency and heat input to calculate thermodynamic power

4. Calculate parasitics and pumping power to calculate net cycle output

5. Calculate the heat to cold TES from constraints. Calculate the total heat from cycle from the efficiency and thermodynamic power. Use these values to calculate the heat rejected to ambient.

Table 16. Cycle Off-Design Inputs and Constraints

Inputs (from system model)	Constraints
Hot TES hot temperature	Cycle controlled to achieve design hot TES cold temperature
Hot HTF mass flow rate	Cycle controlled to achieve cold TES hot temperature
Cold TES cold temperature	Ratio of cold HTF mass flow to hot HTF mass flow is equal to design ratio

$$part\ load\ adjustment = \left(1.0 - \mathbf{abs}\left(1 - \frac{\dot{q}_{hot\ off-design}}{\dot{q}_{hot\ design}}\right)\right)^{0.2} \quad (3)$$

3.8.3 PTES Heat Pump Design-Point and Off-Design Models

The same as the cycle model, we use additional design parameters and the system design-point to fully define the heat pump, as shown in Table 17.

Table 17. Overview of Full Heat-Pump Design Calculations

Design Parameter (Input)	Calculated Design Point (output)
Heat output (from System Design calcs)	Heat in (cooling)
Thermodynamic COP of heat	Thermodynamic power in
Heater multiple	Net electric power in
Electric parasitics as fraction of thermodynamic input electric power	Hot and cold HTF mass flow rates
Hot and cold TES cold and hot tank temperatures	Hot and cold HTF pumping power

Design Parameter (Input)	Calculated Design Point (output)
Hot and cold HTF properties	Carnot COP
Hot and cold HTF pumping power coefficients (kWe/kg/s)	

We model the heat pump off-design performance as a function of hot TES cold temperature, hot HTF mass flow rate, and cold TES hot temperature. The heat pump model is constrained such that the hot TES hot temperature returns at its design temperature. Given these inputs and constraints, summarized in Table 18, cycle performance is calculated as follows:

1. Guess cold TES cold temperature
2. Scale design COP by the product of:
    a. Ratio of design to off-design Carnot efficiency
    b. Part-load non-dimensional adjustment shown in Equation (3)
3. Calculate thermodynamic power input and heat output from heat input and off-design COP
4. Calculate new cold TES cold temperature from calculated heat output, cold TES hot temperature, and cold HTF mass flow rate
5. Compare calculated and guess values of cold TES cold temperature. If values are within a convergence tolerance, then off-design model is converged. Otherwise, iterate at Step 1.

Table 18. Heat Pump Off-Design Inputs and Constraints

Inputs (from system model)	Constraints
Hot TES cold temperature	Heat pump controlled to achieve design hot TES hot temperature
Hot HTF mass flow rate	Ratio of cold HTF mass flow to hot HTF mass flow is equal to design ratio
Cold TES hot temperature	-

3.8.4 PTES System and Dispatch Models

We leveraged the plant controller and numerical convergence models used in many of CSP models and the ETES model as the framework for the PTES system model. Because the PTES interacts with cold TES, we added information flow in the energy and mass balances to pass cold TES information to the cycle and heat pump. The numerical convergence model also calls the two-tank mixed-tank energy balance using temperatures and mass flow rates from the cycle and heat pump models. The PTES model uses the dispatch optimization formulation described above.

3.8.5 Implementation in the SAM User Interface and Scripting

We developed full scripting capabilities for the model by moving all the system design calculations inside of the call to the performance model. In this way, the model does not rely on inputs calculated by the SAM User Interface (UI), which in turn require a user to know and script that relationship when calling the model via script. Instead, the stand-alone ETES and PTES models and hybrid MSPT-ETES model complete all design calculations after loading user inputs. This feature should facilitate quicker and more reliable third-party model adoption. We exclusively used the ETES scripting for the dispatch analysis in this report and the analysis in our journal submission [4].

We also developed new technology models in SAM's UI for the stand-alone ETES and PTES models. This effort involved developing UI pages for each component, modifying cost models for both systems, and connecting the annual performance model to NREL's existing "single owner" financial model. The UI layout for both models follows the layout of the MSPT and physical trough models. First, users enter high-level design parameters (e.g., cycle efficiency, heater multiple, hours of storage) on the System Design page. Then, users can enter more granular component design parameters in the respective component design pages. The ETES model is available in the 2021.12.02 SAM release. The PTES model is available as a Beta release upon request and in NREL's open-source SAM and SSC repositories, and we will include it in the next SAM release (likely fall 2022). Figure 19 shows the stand-alone models as options in the Energy Storage category in SAM's technology selection menu.

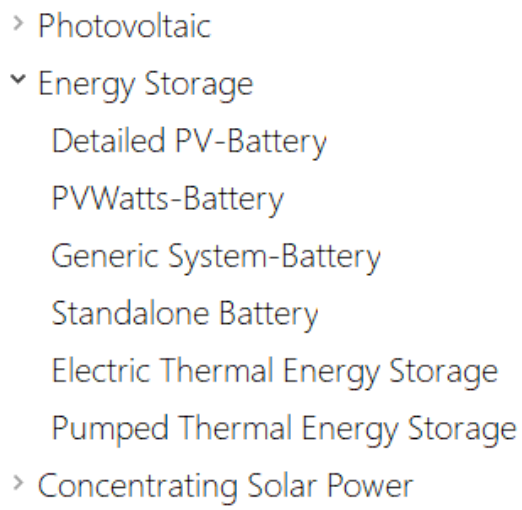

Figure 19. SAM technology selection menu showing stand-alone ETES and PTES models

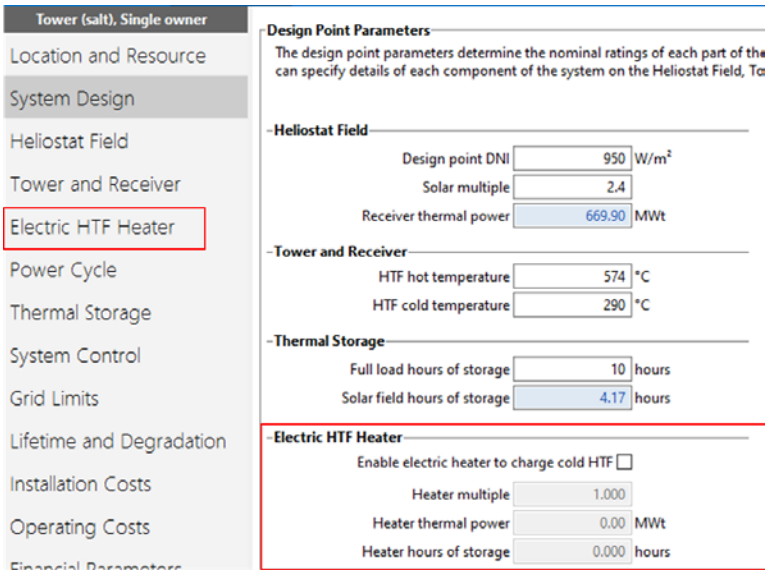

Figure 20. SAM MSPT technology model showing new system design inputs to enable hybrid electric heating and new component page for the electric heater

We added the hybrid MSPT-ETES model as an option within the existing MSPT model in SAM. Figure 20 highlights the primary additions to the MSPT user interface that enable the hybrid ETES option. First, we added a checkbox to the System Design page that enables the heater (default is unchecked). When the heater is selected, the heater design parameter input boxes are enabled. We also added a new component page for the electric heater that lets the user enter heater startup and operational parameters. Finally, we added heater costs to the system costs tabulation in the Installation Costs page.

Dispatch decisions require knowing the absolute electricity price, which in turn requires a known base PPA price. Historically, SAM has provided an option for the user to solve for the base PPA price that achieves a target IRR. The code that solves for this base PPA price is located downstream of the performance model, and as such assumes that the base PPA price does not influence plant performance. To address this, we removed from the stand-alone ETES and PTES models the ability to solve for the base PPA. As a result, the model requires that the user provide the base PPA and calculates the IRR.

Stand-alone grid batteries (i.e., not hybridized with a generator like CSP) result in negative net generation, because they have a round-trip efficiency less than 100%. However, SAM's LCOE calculation and multiple metrics in its cash flow were not designed for negative generation. LCOE uses net generation in the denominator, which would result in a negative LCOE for a grid battery. While it is true that the net energy is negative, a negative LCOE is not a very interesting metric. Additionally, some financial model calculations like O&M costs and incentives are calculated as a function of generation. Consequently, our project team and the larger SAM team modified LCOE calculations so that the denominator instead reflects energy *sales* to the grid and the numerator includes the cost of purchasing electricity from the grid to charge the system.

4 Path Forward

As noted in the PTES section, there are many proposed configurations of PTES, and we designed the PTES model in a general way to capture first order component and system effects. However, it is important to add more detail to this model to better understand how design parameters like cold and hot TES temperatures influence heat pump and cycle performance. Similarly, replacing the heat pump and cycle thermodynamic off-design scaling models with off-design data from a more detailed PTES model will provide a sanity check on the scaling models and ensure that the system control and numerical models are robust. NREL's FY22 Systems Analysis project has a task to use this PTES model as a baseline to study the techno-economics of an air-Brayton PTES system. As part of that task, we will construct a SAM PTES case that models the system with higher resolution.

There is uncertainty about how to define financial inputs, especially for analyses that may want to use a common representative case (as opposed to an ETES company analyzing a particular location for a customer with more clearly defined incentives and constraints). For example, the electricity price signal is one of the most important model inputs. Researchers project that ETES may be competitive at storage durations greater than six hours; however, the electricity pricing on a grid that values this mid-duration storage likely is different than current prices. Consequently, it can be helpful to use modeled future grid pricing, but this raises questions about where to get modeled data and how to understand what it represents. We currently recommend that users explore NREL's Cambium database to get modeled prices from different scenarios, but this tool imposes another learning curve on the user and can flatten price signals relative to prices from higher-fidelity PLEXOS grid scenarios. Similarly, there is uncertainty about revenue streams accessible to ETES beyond arbitrage. SAM can model capacity payments in a relatively simple way; however, it is unclear whether (1) whatever constraints required to collect capacity payments in a specific market need to be considered in the system dispatch and operation, and (2) there are additional revenue streams that should be captured in the financial model.

Finally, multiple stakeholders expressed interest in performance and dispatch models of hybrid systems that combine one or more variable renewable energy resources with ETES. One scenario is to operate the hybrid system as a dispatchable generator where the ETES is charged primarily by the variable renewable energy generator rather than the grid. In this case, the dispatch objective may be to achieve a requested or planned plant output, while satisfying constraints imposed by the variable renewable energy.

5 Publications, Conference Presentations, and Software

Journal Submittals

W. T. Hamilton and T. W. Neises, "Dispatch Optimization of Electric Thermal Energy Storage within System Advisor Model," *Submitt. to Appl. Energy*, 2022.

Conference Presentations

W. T. Hamilton, T. W. Neises, and J. McTigue, "Dispatch Optimization of Grid-scale, Stand-alone Electric Thermal Energy Storage," ASME ES 2021 15th International Conference on Energy Sustainability, Virtual Presentation. 2021.

Software

System Advisor Model version 2021.12.02 [9]

6 References

[1] M. J. Wagner, A. M. Newman, W. T. Hamilton, and R. J. Braun, "Optimized dispatch in a first-principles concentrating solar power production model," *Appl. Energy*, vol. 203, pp. 959–971, 2017, doi: 10.1016/j.apenergy.2017.06.072.

[2] Exemplar Energy, "PLEXOS integrated energy model." https://energyexemplar.com/.

[3] M. J. Wagner, W. T. Hamilton, A. Newman, J. Dent, C. Diep, and R. Braun, "Optimizing dispatch for a concentrated solar power tower," *Sol. Energy*, vol. 174, no. June, pp. 1198–1211, 2018, doi: 10.1016/j.solener.2018.06.093.

[4] W. T. Hamilton and T. W. Neises, "Dispatch Optimization of Electric Thermal Energy Storage within System Advisor Model," *Submitt. to Appl. Energy*, 2022.

[5] G. Brinkman, J. Jorgenson, A. Ehlen, and J. H. Caldwell, "Low Carbon Grid Study: Analysis of a 50% Emission Reduction in California," 2016. [Online]. Available: http://www.nrel.gov/docs/fy16osti/64884.pdf.

[6] J. Mctigue, "Integrated heat pump thermal storage and power cycle for CSP. Final technical report for award DE-EE00034243," 2020.

[7] B. Frew *et al.*, "Impact of operating reserve rules on electricity prices with high penetrations of renewable energy," *Energy Policy*, vol. 156, no. August 2020, p. 112443, 2021, doi: 10.1016/j.enpol.2021.112443.

[8] J. Martinek, J. Jorgenson, M. Mehos, and P. Denholm, "A comparison of price-taker and production cost models for determining system value , revenue , and scheduling of concentrating solar power plants," *Appl. Energy*, vol. 231, no. September, pp. 854–865, 2018, doi: 10.1016/j.apenergy.2018.09.136.

[9] National Renewable Energy Laboratory, "System Advisor Model Version 2021.12.02." 2021, [Online]. Available: https://sam.nrel.gov/download.html.

Appendix A: Hybrid ETES-MSPT Plant Controller Diagrams